AFRL-RV-PS-
TR-2013-0041

AFRL-RV-PS-
TR-2013-0041

DATA ASSOCIATION ALGORITHMS FOR TRACKING SATELLITES

Brandon A. Jones, et al.

Regents of the University of Colorado
3100 Marine Street 572 UCB
Boulder, CO 80309-1058

27 Mar 2013

Final Report

AIR FORCE RESEARCH LABORATORY
Space Vehicles Directorate
3550 Aberdeen Ave SE
AIR FORCE MATERIEL COMMAND
KIRTLAND AIR FORCE BASE, NM 87117-5776

DTIC COPY
NOTICE AND SIGNATURE PAGE

This report is the result of contracted fundamental research deemed exempt from public affairs security and policy review in accordance with SAF/AQR memorandum dated 10 Dec 08 and AFRL/CA policy clarification memorandum dated 16 Jan 09. This report is available to the general public, including foreign nationals. Copies may be obtained from the Defense Technical Information Center (DTIC) (http://www.dtic.mil).

AFRL-RV-PS-TR-2013-0041 HAS BEEN REVIEWED AND IS APPROVED FOR PUBLICATION IN ACCORDANCE WITH ASSIGNED DISTRIBUTION STATEMENT

//SIGNED//
THOMAS LOVELL
Program Manager

//SIGNED//
BRETT J. DEBLONK, Ph.D.
Technical Advisor, Spacecraft Component Technology Branch

//SIGNED//
CHRISTOPHER D. STOIK, Lt Col, USAF
Deputy Chief, Spacecraft Technology Division
Space Vehicles Directorate

REPORT DOCUMENTATION PAGE

Form Approved
OMB No. 0704-0188

1. REPORT DATE *(DD-MM-YY)*	2. REPORT TYPE	3. DATES COVERED *(From - To)*
27-03-2013	Final Report	11 Sep 2008 – 1 Jan 2013

4. TITLE AND SUBTITLE
Data Association Algorithms for Tracking Satellites

5a. CONTRACT NUMBER
FA9453-08-C-0165

5b. GRANT NUMBER

5c. PROGRAM ELEMENT NUMBER
62601F

6. AUTHOR(S)
Brandon A. Jones, Gabriel C. LoDolce, Ben K. Bradley, and George H. Born

5d. PROJECT NUMBER
8809

5e. TASK NUMBER
PPM00004310

5f. WORK UNIT NUMBER
EF004320

7. PERFORMING ORGANIZATION NAME(S) AND ADDRESS(ES)
Regents of the University of Colorado
3100 Marine Street 572 UCB
Boulder, CO 80309-1058

8. PERFORMING ORGANIZATION REPORT NUMBER

9. SPONSORING / MONITORING AGENCY NAME(S) AND ADDRESS(ES)
Air Force Research Laboratory
Space Vehicles Directorate
3550 Aberdeen Ave., SE
Kirtland AFB, NM 87117-5776

10. SPONSOR/MONITOR'S ACRONYM(S)
AFRL/RVSV

11. SPONSOR/MONITOR'S REPORT NUMBER(S)
AFRL-RV-PS-TR-2013-0041

12. DISTRIBUTION / AVAILABILITY STATEMENT
Approved for public release; distribution is unlimited.

13. SUPPLEMENTARY NOTES

14. ABSTRACT
This document describes the work performed as part of the Ananke simulation development. The Ananke simulation tool development is a larger project to provide end-to-end space object simulation and characterization to demonstrate the feasibility of such methods. This document describes the orbit propagation tool, CO-TurboProp, used in the Ananke tool. The document describes the addition of higher-fidelity models in CO-TurboProp and validation of the new tools. The description provided here includes the mathematical back ground and description of the models implemented, as well as a definition of the software interface for the larger Ananke tool. Comparisons of the software with semi-analytic techniques and other available high-fidelity propagation tools are also presented, and all tools met all required and expected accuracies.

15. SUBJECT TERMS
Satellite simulation; Data Association; Algorithms; Sensor Management Algorithms; Filtering: Multisensor, Multi-target Tracking; Satellite Tracking Algorithms; Batch Filters

16. SECURITY CLASSIFICATION OF:			17. LIMITATION OF ABSTRACT	18. NUMBER OF PAGES	19a. NAME OF RESPONSIBLE PERSON
a. REPORT	b. ABSTRACT	c. THIS PAGE			Thomas Lovell
Unclassified	Unclassified	Unclassified	Unlimited	36	19b. TELEPHONE NUMBER *(include area code)*

(This page intentionally left blank)

TABLE OF CONTENTS

List of Figures

List of Tables

1 SUMMARY

This document describes the work performed as part of the Ananke simulation development. This work includes the addition of higher-fidelity models in CU-TurboProp and validation of the new tools. The description provided here includes the mathematical background and description of the models implemented, as well as a definition of the software interface for the larger Ananke tool. Comparisons of the software with semi-analytic techniques and other available high-fidelity propagation tools are also presented, and all tools met all required and expected accuracies.

2 INTRODUCTION

This document describes the work performed by the Colorado Center for Astrodynamics Research (CCAR) at the University of Colorado Boulder as part of the Space-Based Search, Detect, Track project. This project assembled tools developed by several organizations to demonstrate the feasibility of resident space object (RSO) characterization using optical observations. This simulation, called Ananke, provides an end-to-end demonstration of the simulation and processing of optical observations of a previously unknown RSO with the final output describing likely properties of the object. For example, the integrated tool may be used to identify an object as an active, nadir-pointing spacecraft, and includes a probability of this result.

As part of the Ananke simulation, CCAR provided the high-fidelity six degree-of-freedom (6-DOF) models used for simulation of the data and in the various filters used to profile the object. This document provides an overview of these tools and describes the work performed as part of the Ananke project. The next section provides an overview of CU-TurboProp and its role in the Ananke simulation. Section 2.2 then summarizes the work performed over the one-year period of performance. Section 3 describes the models added as part of Ananke, while Section 3.12 provides an interface description for the CU-TurboProp software in Anake. Section 4 then presents validation results of software, followed by a summary and description of future work.

2.1 CU-TurboProp for Ananke

First developed in 2006, CU-TurboProp (hereafter referred to as TurboProp) is the principle tool for rapid orbit propagation at CCAR. This software provides a library of functions to quickly propagate precise orbital or surface trajectories in the convenience of the MATLAB and Python programming environments. To speed up the computations, the orbit propagators use initial value ODE solvers coded in the C programming language. The orbit propagators may be called as MATLAB functions through a MEX interface or in Python via the Simplified Wrapper and Interface Generator (SWIG) module. Hence, the user gets both the superior execution speed of C code along with the ease of matrix computations and plotting that come with high level, interpreted languages.

TurboProp was originally written to propagate orbits in the Circular Restricted Three-body Problem and convert them to the Jet Propulsion Laboratory (JPL) ephemeris. Since then, and partially as a part of the Ananke project, capabilities for higher-fidelity, Earth-centered scenarios have been added. This has enabled space situational awareness (SSA) research ongoing at CCAR. This research first came in the form of testing the prototype cubed-sphere model [1, 2], which was designed for space surveillance and reduces the computation requirements of the gravity perturbation

model. Since then, and partially as a part of the Ananke simulation, capabilities for Earth-centered orbits have been expanded.

For the Ananke simulation, CCAR provided a reduced set of TurboProp functions to: (1) streamline the interface, (2) work with MATLAB defined integrators, e.g. `ode45()`, used in Ananke, and (3) provide the necessary inputs to the bidirectional reflectance distribution function (BRDF) model provided by Pacific Defense Solutions (PDS) for Ananke. Figure 1 provides a high-level overview of this interface.

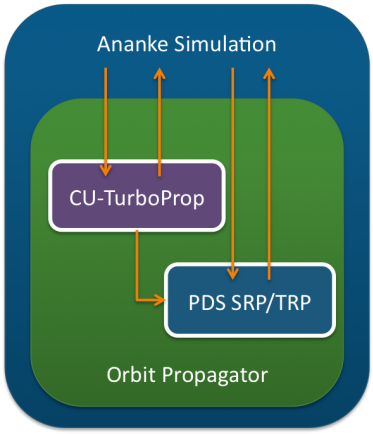

Figure 1. Integration of TurboProp with Ananke

2.2 Work Performed

As part of Ananke, CCAR expanded and updated the suite of models used in TurboProp. Table 1 illustrates the status of the software before and after this project. The improvements to the software are further described in the following sections.

3 METHODS, ASSUMPTIONS, AND PROCEDURES

Orbit propagation incorporating six-degree-of-freedom (6-DOF) modeling requires the computation of modeled accelerations and torques. In this new version of TurboProp, the model is

$$\ddot{\boldsymbol{r}} = \ddot{\boldsymbol{r}}_{\text{2B}} + \ddot{\boldsymbol{r}}_{\text{GP+SET}} + \ddot{\boldsymbol{r}}_{\text{3B}} + \ddot{\boldsymbol{r}}_{\text{Drag}} + \ddot{\boldsymbol{r}}_{\text{SRP}} + \ddot{\boldsymbol{r}}_{\text{ERP}} + \ddot{\boldsymbol{r}}_{\text{GR}} \quad (1)$$

$$\boldsymbol{m} = \boldsymbol{m}_{\text{2B+GP+SET}} + \boldsymbol{m}_{\text{SRP}} \quad (2)$$

where the subscripts indicate the type of acceleration ($\ddot{\boldsymbol{r}}$) or torque ($\boldsymbol{m}$) included in the dynamics. The models implemented in TurboProp include the central body term in the form of the two-body equation (2B), gravity perturbations with a solid Earth tide correction (GP+SET), third-body perturbations (3B), atmospheric drag (Drag), solar radiation pressure (SRP), Earth radiation pressure (ERP), and general relativity (GR). Only some of these terms are included in the torque model. The following sections provide an overview of the models used and developed for the Ananke simulation. Since Ananke only considers objects near geosynchronous orbit, we omit a discussion of atmospheric drag.

Table 1. Overview of Ananke-Derived TurboProp Improvements

Capabilities Before	Capabilities After
• Translational motion • High-fidelity static gravity field • JPL Design Ephemeris • Cannonball Models (drag and SRP) • IAU76/FK6 GCRF/ITRF Model	• Shifted to IERS 2010 Conventions • New/Updated models – 6-DOF (Attitude Dynamics) – Gravity Gradient Torques – Satellite Plate Model – SRP Torques – IAU2006/IAU2000A$_{R06}$ GCRF/ITRF – Solid Earth Tides – Earth Albedo Model – General Relativity Correction • Developed more extensive software validation process • Improved software efficiency for MATLAB interface

Although not immediately apparent in Equations 1 and 2, translation and attitude motion is coupled through the SRP and gravity field. The SRP acceleration is dependent on the orientation of the satellite relative to the satellite-Sun vector. Hence, it depends on the current attitude state. Additionally, the current position of the satellite influences the gravity perturbation and SRP models, creating a dependence on the translation state in attitude dynamics. This illustrates how high-fidelity, 6-DOF modeling of the satellite motion is required for highly accurate state propagation.

3.1 IERS 2010 Conventions

As indicated in Table 1, TurboProp was updated to more closely adhere to the International Earth Rotation and Reference System (IERS) 2010 conventions for orbit propagation [3]. This mainly required an update of the transformation between the Geocentric Celestial Reference Frame (GCRF) and the International Terrestrial Reference Frame (ITRF). More information on this update may be found in Section 3.11. Otherwise, new models included in TurboProp are based on the IERS conventions (where appropriate).

3.2 Central Body Forces

The two-body equation describing the the gravitational forces due to the central body is

$$\ddot{\boldsymbol{r}}_{2\text{B}} = -\frac{\mu}{r^3}\boldsymbol{r} \tag{3}$$

where $\boldsymbol{r}$ is the position vector of the spacecraft with respect to the planet's center of mass, r is the magnitude of that vector, and μ is the gravitational parameter of the central body. In this document

$$\boldsymbol{r} = \begin{bmatrix} x & y & z \end{bmatrix}^T \tag{4}$$

is a position vector with components x, y, and z.

3.3 Central Body Gravity Perturbations

The aspherical gravity field is modeled using U, an aspherical potential function excluding the two-body term [4],

$$U(x,y,z) = \frac{\mu}{r}\sum_{n=2}^{\infty}\sum_{m=0}^{n}\left(\frac{R}{r}\right)^n \bar{A}_{n,m}\left[\frac{z}{r}\right]\{\bar{C}_{n,m}\bar{E}_m + \bar{S}_{n,m}\bar{F}_m\} \tag{5}$$

where

$$\bar{E}_m = \bar{E}_1\bar{E}_{m-1} - \bar{F}_1\bar{F}_{m-1}, \quad \bar{E}_0 = 1, \quad \bar{E}_1 = \frac{x}{r} \tag{6a}$$

$$\bar{F}_m = \bar{F}_1\bar{E}_{m-1} + \bar{E}_1\bar{F}_{m-1}, \quad \bar{F}_0 = 0, \quad \bar{F}_1 = \frac{y}{r}. \tag{6b}$$

We note this form is defined in terms of the Cartesian, not spherical, coordinates. Thus, it does not contain the polar singularity present in the classical formulation presented in [5, 6, 7], and elsewhere. R is the radius of the central body, μ is the gravitational parameter of the central body, and n and m are the degree and order of the spherical harmonic model, respectively. $\bar{C}_{n,m}$ and $\bar{S}_{n,m}$ are the normalized Stokes coefficients describing the magnitude of the spherical harmonic functions, and are specific to the gravity field model being used. $\bar{A}_{n,m}\left[\alpha = \frac{z}{r}\right]$ is a normalized, derived Legendre function computed using the following recursion:

$$\begin{aligned}
\bar{A}_{0,0}[\alpha] &= 1 \\
\bar{A}_{1,0}[\alpha] &= \alpha\sqrt{3} \\
\bar{A}_{1,1}[\alpha] &= \sqrt{3} \\
\bar{A}_{n,n}[\alpha] &= \sqrt{\frac{2n+1}{2n}}\bar{A}_{n-1,n-1}[\alpha] \qquad n > 1 \\
\bar{A}_{n,m}[\alpha] &= \alpha B_{n,m}\bar{A}_{n-1,m}[\alpha] - \frac{B_{n,m}}{B_{n-1,m}}\bar{A}_{n-2,m}[\alpha] \qquad m < n
\end{aligned} \tag{7}$$

where

$$B_{n,m} = \sqrt{\frac{(2n+1)(2n-1)}{(n+m)(n-m)}}. \tag{8}$$

The $B_{n,m}$ and $\frac{B_{n,m}}{B_{n-1,m}}$ coefficients are not a function of α, and are precomputed at software initialization for future use. This formulation of the derived Legendre functions is adapted from personal correspondence with Dr. Bob Schutz of the University of Texas Center for Space Research and from his book Satellite Dynamics: Theory and Application being written with G. Giacaglia. This adaptation to the formulation in Schutz's book was based on [8], and is consistent with [4].

The acceleration in body-fixed coordinates, $\ddot{\boldsymbol{r}}$, is found by taking the gradient of the potential U in Cartesian coordinates. As derived in [4], the following equations summarize the method:

$$a_1 = \sum_{n=2}^{\infty} \left(\frac{R}{r}\right)^n \sum_{m=1}^{n} m\bar{A}_{n,m} \left(C_{n,m}\bar{E}_{m-1} + S_{n,m}\bar{F}_{m-1}\right) \tag{9a}$$

$$a_2 = \sum_{n=2}^{\infty} \left(\frac{R}{r}\right)^n \sum_{m=1}^{n} m\bar{A}_{n,m} \left(S_{n,m}\bar{E}_{m-1} - C_{n,m}\bar{F}_{m-1}\right) \tag{9b}$$

$$a_3 = \sum_{n=2}^{\infty} \left(\frac{R}{r}\right)^n \sum_{m=0}^{n} \bar{A}_{n,m+1}\Gamma_{n,m} \left(C_{n,m}\bar{E}_{m} + S_{n,m}\bar{F}_{m}\right) \tag{9c}$$

$$a_4 = \sum_{n=2}^{\infty} \left(\frac{R}{r}\right)^n \sum_{m=0}^{n} (n+m+1)\bar{A}_{n,m} \left(C_{n,m}\bar{E}_{m} + S_{n,m}\bar{F}_{m}\right) \tag{9d}$$

$$\ddot{\boldsymbol{r}}_{\text{GP}} = -\frac{\mu}{r^2}\left(\left(\frac{z}{r}a_3 + a_4\right)\frac{\boldsymbol{r}}{r} - \begin{bmatrix} a_1 \\ a_2 \\ a_3 \end{bmatrix}\right) \tag{9e}$$

where

$$\Gamma_{n,m} = \Pi_{n,m+1}/\Pi_{n,m} = \sqrt{\frac{(n+m+1)(n-m)(2-\delta_{0m})}{2}} \tag{10}$$

and

$$\Pi_{n,m} = \sqrt{\frac{(n+m)!}{(n-m)!(2-\delta_{0m})(2n+1)}}. \tag{11}$$

In the software, $\Gamma_{n,m}$ is precomputed and stored at initialization.

The equations of motion are integrated in the inertial frame, so the spacecraft state vector must be converted from the inertial frame to the body-fixed frame before computing the accelerations. After computing the body-fixed accelerations, they must be converted back into the inertial frame. The GCRF/ITRF conversion from an inertial to a fixed frame is described in detail in Section 3.11.

When propagating state deviations in the classic linearized filters, the state vector is augmented with a state transition matrix (STM). In such a formulation, the STM $\boldsymbol{\Phi}$ maps a given deviation vector $\boldsymbol{x}_0$ at time t_0 to a given time t_k

$$\boldsymbol{x}_k = \boldsymbol{\Phi}(t_k, t_0)\boldsymbol{x}_0. \tag{12}$$

The state transition matrix is typically propagated simultaneously with the state using

$$\dot{\boldsymbol{\Phi}}(t_k, t_0) = \boldsymbol{A}(t_k)\boldsymbol{\Phi}(t_k, t_0) \tag{13}$$

where

$$\boldsymbol{A}(t) = \frac{\partial \boldsymbol{F}(\boldsymbol{X}, t)}{\partial \boldsymbol{X}(t)}, \tag{14}$$

$\boldsymbol{X}$ is the state vector, and $\boldsymbol{A}$ is of the form

$$\boldsymbol{A} = \begin{bmatrix} \frac{\partial \dot{x}}{\partial x} & \frac{\partial \dot{x}}{\partial y} & \frac{\partial \dot{x}}{\partial z} & \cdots & \frac{\partial \dot{x}}{\partial \dot{z}} \\ \frac{\partial \dot{y}}{\partial x} & \frac{\partial \dot{y}}{\partial y} & \frac{\partial \dot{y}}{\partial z} & & \\ \frac{\partial \dot{z}}{\partial x} & \frac{\partial \dot{z}}{\partial y} & \frac{\partial \dot{z}}{\partial z} & & \vdots \\ \vdots & & & \ddots & \\ \frac{\partial \ddot{z}}{\partial x} & & \cdots & & \frac{\partial \ddot{z}}{\partial \dot{z}} \end{bmatrix}. \tag{15}$$

Although Ananke does not require the STM, the gravity gradient formulation presented in Section 3.9 will require $\boldsymbol{A}$. The remainder of this section presents the mathematical formulation of this matrix.

To include the two-body acceleration in the variational equations used to create matrix $\boldsymbol{A}$, the partials of the two-body portion of $\ddot{\boldsymbol{r}}$ with respect to $\boldsymbol{r}$ are computed in this manner:

$$\boldsymbol{A}_{\text{2B}} = \left[\frac{d\ddot{\boldsymbol{r}}}{d\boldsymbol{r}}\right] = \frac{3\mu}{r^3}\begin{bmatrix} \frac{x^2}{r^2} - \frac{1}{3} & \frac{xy}{r^2} & \frac{xz}{r^2} \\ \frac{xy}{r^2} & \frac{y^2}{r^2} - \frac{1}{3} & \frac{yz}{r^2} \\ \frac{xz}{r^2} & \frac{yz}{r^2} & \frac{z^2}{r^2} - \frac{1}{3} \end{bmatrix}. \tag{16}$$

To include the gravity perturbations in the matrix $\boldsymbol{A}$, the partial of the gravity field portion of $\ddot{\boldsymbol{r}}$ with respect to $\boldsymbol{r}$ is computed. These variational equations were derived in [4], and are provided here as a reference. The resulting matrix is

$$\begin{aligned} \boldsymbol{A}_{\text{GP}} &= \frac{\partial \ddot{\boldsymbol{r}}_{\text{GP}}}{\partial \boldsymbol{r}} && (17) \\ &= \frac{\mu}{r^3}\left\{ \begin{bmatrix} \hat{\boldsymbol{r}} & \hat{k} \end{bmatrix} \begin{bmatrix} F & G \\ G & M \end{bmatrix} \begin{bmatrix} \hat{\boldsymbol{r}}^T \\ \hat{k}^T \end{bmatrix} + \begin{bmatrix} \hat{\boldsymbol{r}} & \boldsymbol{d} \end{bmatrix} \begin{bmatrix} 0 & -1 \\ -1 & 0 \end{bmatrix} \begin{bmatrix} \hat{\boldsymbol{r}}^T \\ \boldsymbol{d}^T \end{bmatrix} \right. \\ &\qquad \left. + \begin{bmatrix} N-\Lambda & -\Omega & Q \\ -\Omega & -(N+\Lambda) & R \\ Q & R & -\Lambda \end{bmatrix} \right\} && (18) \end{aligned}$$

where

$$\begin{aligned} \epsilon &= \frac{z}{r} && (19) \\ \hat{k} &= \begin{bmatrix} 0 & 0 & 1 \end{bmatrix}^T && (20) \\ \boldsymbol{d} &= \epsilon \begin{bmatrix} Q & R & 0 \end{bmatrix}^T + \begin{bmatrix} S & T & 0 \end{bmatrix}^T && (21) \\ \Lambda &= (\epsilon a_3 + a_4) && (22) \\ F &= L + \epsilon(M\epsilon + 2(P + a_3)) + \Lambda && (23) \\ G &= -(M\epsilon + P + a_3). && (24) \end{aligned}$$

Additionally,

$$L = \sum_{n=2}^{\infty}\left(\frac{R}{r}\right)^n \sum_{m=0}^{n}(n+m+1)(n+m+2)\bar{A}_{n,m}(\bar{C}_{n,m}\bar{E}_m + \bar{S}_{n,m}\bar{F}_m) \tag{25}$$

$$M = \sum_{n=2}^{\infty}\left(\frac{R}{r}\right)^n \sum_{m=0}^{n}\bar{A}_{n,m+2}\Psi_{n,m}(\bar{C}_{n,m}\bar{E}_m + \bar{S}_{n,m}\bar{F}_m) \tag{26}$$

$$N = \sum_{n=2}^{\infty}\left(\frac{R}{r}\right)^n \sum_{m=2}^{n}m(m-1)\bar{A}_{n,m}(\bar{C}_{n,m}\bar{E}_{m-2} + \bar{S}_{n,m}\bar{F}_{m-2}) \tag{27}$$

$$\Omega = \sum_{n=2}^{\infty}\left(\frac{R}{r}\right)^n \sum_{m=2}^{n}m(m-1)\bar{A}_{n,m}(\bar{C}_{n,m}\bar{F}_{m-2} - \bar{S}_{n,m}\bar{E}_{m-2}) \tag{28}$$

$$P = \sum_{n=2}^{\infty}\left(\frac{R}{r}\right)^n \sum_{m=0}^{n}(n+m+1)\bar{A}_{n,m+1}\Gamma_{n,m}(\bar{C}_{n,m}\bar{E}_m + \bar{S}_{n,m}\bar{F}_m) \tag{29}$$

$$Q = \sum_{n=2}^{\infty}\left(\frac{R}{r}\right)^n \sum_{m=1}^{n}m\bar{A}_{n,m+1}\Gamma_{n,m}(\bar{C}_{n,m}\bar{E}_{m-1} + \bar{S}_{n,m}\bar{F}_{m-1}) \tag{30}$$

$$R = \sum_{n=2}^{\infty}\left(\frac{R}{r}\right)^n \sum_{m=1}^{n}m\bar{A}_{n,m+1}\Gamma_{n,m}(\bar{S}_{n,m}\bar{E}_{m-1} - \bar{C}_{n,m}\bar{F}_{m-1}) \tag{31}$$

$$S = \sum_{n=2}^{\infty}\left(\frac{R}{r}\right)^n \sum_{m=1}^{n}(n+m+1)m\bar{A}_{n,m}(\bar{C}_{n,m}\bar{E}_{m-1} + \bar{S}_{n,m}\bar{F}_{m-1}) \tag{32}$$

$$T = \sum_{n=2}^{\infty}\left(\frac{R}{r}\right)^n \sum_{m=1}^{n}(n+m+1)m\bar{A}_{n,m}(\bar{S}_{n,m}\bar{E}_{m-1} - \bar{C}_{n,m}\bar{F}_{m-1}). \tag{33}$$

Note the equation for S corrects a mistake in [4]. Finally,

$$\Psi_{n,m} = \Pi_{n,m+2}/\Pi_{n,m} = \sqrt{\frac{(n+m+1)(n+m+2)(n-m)(n-m-1)(2-\delta_{m,0})}{2}}. \tag{34}$$

Once the matrix $\boldsymbol{A}_{\text{GP}}$ is computed, it must be rotated from the Earth-fixed frame to the inertial frame before being added to $\boldsymbol{A}_{\text{2B}}$. This is done with the Earth-fixed to inertial rotation matrix $\boldsymbol{T}_i^e$ described in Section 3.11. Hence,

$$\boldsymbol{A} = \boldsymbol{A}_{\text{2B}} + [\boldsymbol{A}_{\text{GP}}]_i = \boldsymbol{A}_{\text{2B}} + [\boldsymbol{T}_i^e]^T [\boldsymbol{A}_{\text{GP}}]_e [\boldsymbol{T}_i^e]. \tag{35}$$

The gravity model used in TurboProp still requires a definition of the Stokes coefficients $\bar{C}_{n,m}$ and $\bar{S}_{n,m}$. These coefficients are provided through a text file, with several options provided with the software. For Earth-centered orbits, we provide the GGM03C (`GGM03C.sha`) [9], EGM2008 (tide-free: `EGM2008tf.sha`, zero-tide: `EGM2008zt.sha`) [10], EGM98 (`EGM98.sha`) [11], JGM-3 (`JGM3.sha`) [12], and WGS-84 (`WGS84.sha`) [13] gravity models. We note that the values of μ and R used in the spherical harmonic model must match those dictated by the model.

The gravity field format was based on the file format for the lunar gravity field `jgl100k1.sha` found at

`http://pds-geosciences.wustl.edu/missions/lunarp/shadr.html`

Table 2. Header Line Format for Gravity Field Files

C format string: `" %le, %le, %le, %d, %d, %d, %le, %le"`		
Parameter Description	Format	Units
Reference radius of the planet	Scientific notation	km
Gravitational parameter	Scientific notation	km^3/sec^2
Gravitational parameter uncertainty	Scientific notation	km^3/sec^2 (discarded)
Degree of model field	Integer	N/A (discarded)
Order of model field	Integer	N/A (discarded)
Normalization	Integer	0 = unnormalized 1 = normalized
Reference longitude, normally 0	Scientific notation	degrees (discarded)
Reference latitude, normally 0	Scientific notation	degrees (discarded)

The first line is a header and contains eight parameters, three of which are used and the rest discarded. The parameters are shown in Table 2.

Note that these parameters are comma-delimited. If `extras.mu` was not input by the user, the gravitational parameter and reference radius from this header line will be used for all gravity calculations for the central body. The user can provide `extras.mu` and `extras.radius` to override the parameters in the gravity header line. Since these values are dictated by the model selected, e.g., GGM02C, this input should only be used to change the length or time units to match those of the propagated state.

After the header line, "data lines" contain the gravity field coefficients. These coefficients are also comma-delimited also, and are described in Table 3.

Table 3. Data Line Format for Gravity Field Files

C format string: `" %d, %d, %le, %le, %le, %le"`	
Parameter Description	Format
Degree index n	Integer
Order index m	Integer
Coefficient $C_{n,m}$	Scientific Notation
Coefficient $S_{n,m}$	Scientific Notation
Uncertainty in coefficient $C_{n,m}$	Scientific Notation
Uncertainty in coefficient $S_{n,m}$	Scientific Notation

3.4 Solid Earth Tides

The solid Earth tide model now implemented in TurboProp uses the formulation presented in the IERS 2010 conventions [3]. The SET perturbations account for temporal variations in the mass distribution of the solid Earth due to other planetary bodies (Moon, Sun, etc.). It does not account for variations in the liquid distribution (oceans, etc.), which would be handled by a liquid Earth tide

model. The theory behind such models is extensive, and beyond the scope of this document. In the interest of brevity, we only provide a high-level overview of the SET model with key equations to aid in understanding the elements of its computation.

When augmenting the spherical harmonic model presented in Section 3.3 to account for temporal variations, the SET model simply perturbs the Stokes coefficients

$$\bar{C}_{n,m} = \bar{C}_{n,m} + \Delta\bar{C}_{n,m}, \qquad \bar{S}_{n,m} = \bar{S}_{n,m} + \Delta\bar{S}_{n,m}, \tag{36}$$

where the deviations $\Delta\bar{C}_{n,m}$ and $\Delta\bar{S}_{n,m}$ are determined by the model. The acceleration vector $\ddot{\boldsymbol{r}}_{\text{GP+SET}}$ and the variational equations $\boldsymbol{A}_{\text{2B+GP+SET}}$ are found by evaluating Equations 9e and 18 with the corrected coefficients. The temporal changes are modeled using several terms, including variations in the pole of rotation, secular variations in the low-degree coefficients, frequency-dependent effects, and others. Secular variations, although not strictly a part of the SET model, are modeled using

$$\bar{C}_{n,0}(t) = \bar{C}_{n,0}(t_0) + \dot{\bar{C}}_{n,0}(t - t_0) \tag{37}$$

where the secular rates $\dot{\bar{C}}_{n,0}$ and epoch times t_0 are provided in Table 4 (adapted from Table 6.2 of [3]). The remainder of the current SET model is a three step process:

1. Evaluate the frequency-independent terms modifying the (n, m) coefficients for $n = 0, \ldots, 4$.
2. Generate corrections due to the frequency-dependent contributions in the $(2, m)$, $m = 0, 1, 2$ terms.
3. If required, remove the permanent tide correction.

After computing the corrections $\Delta C^{(i)}_{n,m}$ and $\Delta S^{(i)}_{n,m}$ for steps $i = 1, 2, 3$, the final correction is simply the sum over i.

Table 4. Secular Gravity Field Variations [3]

Coefficient	Value at J2000.0	Rate / yr^{-1}
$\bar{C}_{2,0}$	-0.48416948$\times10^{-3}$	11.6$\times10^{-12}$
$\bar{C}_{3,0}$	0.9571612$\times10^{-6}$	4.9$\times10^{-12}$
$\bar{C}_{4,0}$	0.5399659 $\times10^{-6}$	4.7$\times10^{-12}$

The Step 1 corrections depend on the position of any perturbing third bodies, usually the Sun and Moon. Mathematically, the corrections $\Delta\bar{C}^{(1)}_{n,m}$ and $\Delta\bar{S}^{(1)}_{n,m}$ for the $n = 2, 3$ terms are

$$\begin{bmatrix} \Delta\bar{C}^{(1)}_{n,m} \\ \Delta\bar{S}^{(1)}_{n,m} \end{bmatrix} = \frac{k_{n,m}}{2n+1} \sum_p \frac{\mu_p}{\mu_\oplus} \left(\frac{R_\oplus}{r_p}\right)^{n+1} \bar{P}_{n,m}\left[\sin\phi_p\right] \begin{bmatrix} \cos(m\lambda_p) \\ \sin(m\lambda_p) \end{bmatrix} \tag{38}$$

where $k_{n,m}$ is the nominal Love number for degree n and order m, r_p is the distance from the Earth to the third body (computed using the JPL design ephemeris), μ_p is the third body gravitation parameter, $\bar{P}_{n,m}$ is the associated Legendre function, ϕ_p and λ_p are the geocentric latitude and longitude of the third body, and p is the index of summation over the third-bodies considered in

the model. The '$\oplus$' subscript indicates a parameter for the Earth. For the $n = 4, m = 0, 1, 2$ coefficients,

$$\begin{bmatrix} \Delta\bar{C}^{(1)}_{4,m} \\ \Delta\bar{S}^{(1)}_{4,m} \end{bmatrix} = \frac{k^{(+)}_{2,m}}{5} \sum_p \frac{\mu_p}{\mu_\oplus} \left(\frac{R_\oplus}{r_p}\right)^3 \bar{P}_{2,m}\left[\sin\phi_p\right] \begin{bmatrix} \cos(m\lambda_p) \\ \sin(m\lambda_p) \end{bmatrix} \tag{39}$$

where $k^{(+)}_{2,m}$ accounts for anelasticity of the Earth. The values for $k_{n,m}$ and $k^{(+)}_{2,m}$ may be found in Table 6.3 of [3].

In Step 2 of the SET model, we generate the frequency-dependent contributions. For the $(2, 0)$ term

$$\Delta\bar{C}^{(2)}_{2,0} = \sum_{f(2,0)} \left(I_{f(2,0)} \cos(\theta_{f(2,0)}) - O_{f(2,0)} \sin(\theta_{f(2,0)})\right) \tag{40}$$

where $I_{f(2,0)}$ and $O_{f(2,0)}$ are the in-phase and out-of-phase amplitudes for each of the tides $f(2, 0)$. Example $f(2, 0)$ tides include, but are not limited to, the S_a and M_m tides. $\theta_{f(2,0)}$ is defined on p. 84 of [3], which is a function of the Greenwich Mean Sidereal time, the fundamental arguments of nutation theory, and the multipliers of these arguments for the tide $f(2, 0)$. A list of the tides, the amplitudes, and the vector multipliers for the $(2, 0)$ correction may be found in Table 6.5b of [3]. Using the values for the amplitudes given in Tables 6.5a and 6.5c of [3], the corrections to the $(2, 1)$ and $(2, 2)$ terms are

$$\begin{bmatrix} \Delta\bar{C}^{(2)}_{2,1} \\ \Delta\bar{S}^{(2)}_{2,1} \end{bmatrix} = \sum_{f(2,1)} \begin{bmatrix} I_{f(2,1)} \sin(\theta_{f(2,1)}) + O_{f(2,1)} \cos(\theta_{f(2,1)} \\ I_{f(2,1)} \cos(\theta_{f(2,1)}) - O_{f(2,1)} \sin(\theta_{f(2,1)}) \end{bmatrix} \tag{41}$$

$$\begin{bmatrix} \Delta\bar{C}^{(2)}_{2,2} \\ \Delta\bar{S}^{(2)}_{2,2} \end{bmatrix} = \sum_{f(2,2)} \begin{bmatrix} I_{f(2,2)} \cos(\theta_{f(2,2)}) \\ -I_{f(2,2)} \sin(\theta_{f(2,2)}) \end{bmatrix}. \tag{42}$$

Finally, Step 3 removes the permanent tide correction from the $C_{2,0}$ term, if required. *Zero tide* models of the gravity field include a correction for the permanent tide already accounted for in Steps (1) and (2). Hence, this correction must be removed to prevent its duplication. This correction is dependent on the model, and is not necessary when using a *tide free* model.

Although not described here, the TurboProp implementation also includes corrections for the solid and ocean pole tides. More information on these corrections may be found in Sections 6.4 and 6.5 of [3].

3.5 JPL Design Ephemeris

The JPL planetary ephemeris model (DE) expresses the location of third bodies, e.g., the Moon or Sun, in the ICRF inertial reference frame centered on a user-specified central body. Upon centering the location relative to the Earth, the positions are expressed in the GCRF frame. The positions and velocities of all the planets are obtained from JPL DE ephemerides: DE403 [14], DE405 [15], or DE421 [16]. The numeric value in the name is a version number, with DE421 being the most recent publicly available version. After software installation, the binary ephemeris files for DE403 and DE405 are called `DE.403` and `DE.404`, respectively. Although not included in the final release of TurboProp for the Ananke simulation, CCAR completed the integration of the updated DE421 towards the end of the Ananke work period.

The code used to create the ephemeris files and to perform the interpolation was adapted from work by CCAR graduate student Greg Lehr and code by Mark Hoffman at

`ftp://ssd.jpl.nasa.gov/pub/eph/planets/C-versions/hoffman/`

The ephemeris data files were obtained from

`ftp://ssd.jpl.nasa.gov/pub/eph/planets/ascii`

Using the DE-determined position of any perturbing bodies, the third-body accelerations are then [5]

$$\ddot{\boldsymbol{r}}_3 = -\mu_3 \left(\frac{\boldsymbol{r}_{3,s}}{r_{3,s}^3} + \frac{\boldsymbol{r}_{c,3}}{r_{c,3}^3} \right), \tag{43}$$

where μ_3 is the gravitational parameter of the third-body, $\boldsymbol{r}_{3,s}$ is the vector from the third-body to the satellite, $\boldsymbol{r}_{c,3}$ is the vector from the central body to the third-body, and $r_{3,s}$ and $r_{c,3}$ are the vector magnitudes. By default, the gravitational parameters are taken from the JPL ephemeris. The total perturbation $\ddot{\boldsymbol{r}}_{3\text{B}}$ is then the sum of the accelerations for each third-body included in the model.

3.6 Earth Radiation Pressure Model

The Earth radiation pressure model (ERP) implemented in TurboProp uses the formulation presented in [17]. Not much research has been conducted in the field of ERP, and this model appears to be the one most commonly employed in the literature. In summary, the model determines the region of the Earth visible to the satellite as a function of its Earth-centered position. The visible area is then segmented into N elements, each with some surface area A_j. This segmentation is illustrated in Figure 2. The acceleration imparted on the satellite is then computed for each element, with the sum of these vectors yielding the total ERP perturbation. The Earth albedo and emissivity, a_j and e_j (for element j) accounts for seasonal variations using the low-degree Legendre polynomial interpolation

$$a_j = 0.34 + 0.10\cos(\omega(t - t_0))P_1(\sin(\phi_j)) + 0.29P_2(\sin(\phi_j)) \tag{44}$$

$$e_j = 0.68 - 0.07\cos(\omega(t - t_0))P_1(\sin(\phi_j)) - 0.18P_2(\sin(\phi_j)) \tag{45}$$

where the coefficients are the empirical values presented in [17], $P_n(\sin(\phi_j))$ is the n-th degree Legendre polynomial, ϕ_j is the equatorial latitude for the center of element j, ω is the Earth's orbit mean motion ($\approx 2\pi/365.25$ rad/yr), and t_0 is the epoch Dec 22, 1981. With these parameters, the ERP acceleration according to [17] is then

$$\ddot{\boldsymbol{r}}_{\text{ERP}} = \sum_{j=1}^{N} \ddot{\boldsymbol{r}}_j \tag{46}$$

where

$$\ddot{\boldsymbol{r}}_j = \frac{C_R A_s}{cM\pi} \left((\tau a_j I_\odot \cos(\theta_{S_j}) + e_j E_\oplus) \frac{\cos(\alpha_j) A_j}{r_j^2} \right) \hat{\boldsymbol{r}}, \tag{47}$$

τ is zero or one if the center of the element is in shadow or illuminated, respectively, c is the speed of light, $I_\odot$ is the local solar irradiance for the element, C_R, M, and A_s are the satellite's coefficient

of reflectivity, mass and area, respectively, $E_\oplus$ is the exitance of the Earth, and r_j is the element-to-satellite distance. We note that the presentation here expresses the equations in the inertial frame. For visible elements, i.e., $\cos(\alpha_j) \neq 0.0$, Equation 47 is nonzero if the element is not illuminated. This describes the force imparted on the satellite due to continued energy emission of the shaded portion of the Earth.

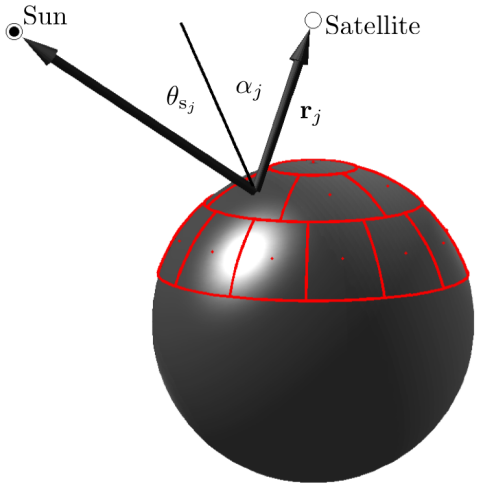

Figure 2. Vector geometry of the TurboProp ERP model

3.7 General Relativity Correction

The equations for gravitational forces discussed in previous sections obey Newtonian mechanics, but high-precision propagation requires a treatment defined by the theory of general relativity (GR). The IERS 2010 conventions define a correction for the effects of GR formulated using three principle terms [3, Equation 10.12]. The Schwarzschild term is several orders of magnitude greater than the other two. Since the contribution of the GR correction is already on the order of 10^{-9} in low Earth orbit when compared to the two-body term, we truncate the smaller terms. This is further justified since the relative accuracy of the gravity field does not exceed 10^{-9}. The correction for GR in TurboProp is then

$$\ddot{\boldsymbol{r}}_{\text{GR}} = \frac{\mu_\oplus}{c^2 r^3}\left[\left(4\frac{\mu_\oplus}{r} - \dot{\boldsymbol{r}}\cdot\dot{\boldsymbol{r}}\right)\boldsymbol{r} + 4\left(\boldsymbol{r}\cdot\dot{\boldsymbol{r}}\right)\dot{\boldsymbol{r}}\right]. \tag{48}$$

3.8 Modeling 6-DOF Motion

High-fidelity propagation of a satellite state requires properly accounting for the coupled translation and attitude states. To this end, TurboProp now offers a capability to propagate a satellite state with these additional degrees of freedom. TurboProp uses a quaternion ($\vec{q}_b^{\,i}$) formulation to represent the coordinate rotation from the inertial (i) to the satellite body frame (b), and includes propagation of the angular rates based on a given torque vector ($\boldsymbol{m}$). This section describes the formulation of the attitude dynamics.

Propagation of the quaternion is modeled as a composition of the initial quaternion and a small rotation. Given the initial quaternion $\bar{q}_b^i$,

$$\dot{\bar{q}} = \begin{bmatrix} \dot{q}_0 \\ \dot{\boldsymbol{q}} \end{bmatrix} = \bar{q}_b^i \otimes \bar{\omega} = \frac{1}{2} \begin{bmatrix} 0 & -\delta\omega_1 & -\delta\omega_2 & -\delta\omega_3 \\ \delta\omega_1 & 0 & \delta\omega_3 & -\delta\omega_2 \\ \delta\omega_2 & -\delta\omega_3 & 0 & \delta\omega_1 \\ \delta\omega_3 & \delta\omega_2 & -\delta\omega_1 & 0 \end{bmatrix} \begin{bmatrix} q_0 \\ \boldsymbol{q} \end{bmatrix} \tag{49}$$

where $\bar{\omega}$ is the pure quaternion generated by infinitesimal angular rate vector $\delta\boldsymbol{\omega}$. We note that, for notation purposes, we include the scalar portion of the quaternion first as q_0, followed by the vector portion $\boldsymbol{q}$. More information on quaternions may be found in [18] or [19].

Propagation of the angular rates uses the Euler rotational equations of motion [18]

$$\boldsymbol{J}\dot{\boldsymbol{\omega}} = \boldsymbol{m} - \boldsymbol{\omega} \times \boldsymbol{J}\boldsymbol{\omega} \tag{50}$$

where $\boldsymbol{J}$ is the moment of inertia tensor, $\boldsymbol{\omega}$ is the rotation vector for the satellite in the body frame, and $\boldsymbol{m}$ is the vector of torques in the body frame. The vector of body rotation rates $\boldsymbol{\omega}$ are also expressed in the body frame. Assuming that no changes to the satellite's mass distribution are modeled, the tensor $\boldsymbol{J}^{-1}$ may be precomputed at initialization. The torques computed as part of TurboProp are described in the following sections.

3.9 Gravity Gradient Torques

The previous description propagates the rotational states of a given satellite when given the torques $\boldsymbol{m}$. In TurboProp, the torques can include those due to gravity gradient effects. The full central-body gravity model uses the spherical harmonic model previously described in Section 3.3. Also included in this derivative function are gravity gradient torques. As described in [4], the gravity gradient torques may be written in terms of the variational equations

$$\boldsymbol{m}_{\text{2B+GP+SET}} = \begin{bmatrix} \mathcal{A}_{23}(J_{33} - J_{22}) - \mathcal{A}_{13}J_{12} + \mathcal{A}_{12}J_{13} - J_{23}(\mathcal{A}_{33} - \mathcal{A}_{22}) \\ \mathcal{A}_{13}(J_{11} - J_{33}) + \mathcal{A}_{23}J_{12} - \mathcal{A}_{12}J_{23} - J_{13}(\mathcal{A}_{11} - \mathcal{A}_{33}) \\ \mathcal{A}_{12}(J_{22} - J_{11}) - \mathcal{A}_{23}J_{13} + \mathcal{A}_{13}J_{23} - J_{12}(\mathcal{A}_{22} - \mathcal{A}_{11}) \end{bmatrix} \tag{51}$$

where

$$\boldsymbol{\mathcal{A}} = [\boldsymbol{A}_{\text{2B+GP+SET}}]_b = \boldsymbol{T}_b^i \left(\boldsymbol{T}_i^e \left[\boldsymbol{A}_{\text{GP+SET}} \right]_e \boldsymbol{T}_e^i + \boldsymbol{A}_{\text{2B}} \right) \boldsymbol{T}_i^b, \tag{52}$$

i.e., the gravity field variational equations (including the two-body term) in the satellite body-fixed frame. The variables J_{mn} and $\mathcal{A}_{nm}$ refer to the element in the n-th row and m-th column of the $\boldsymbol{J}$ and $\boldsymbol{\mathcal{A}}$ matrices, respectively. The matrices $\boldsymbol{A}_{\text{GP}}$ and $\boldsymbol{A}_{\text{GP+SET}}$ were previously defined in Section 3.3. The rotation matrix $\boldsymbol{T}_b^i$ may be computed from $\bar{q}_b^i$, and $\boldsymbol{T}_i^e$ is given by the orientation parameters (see Sections 3.11 and 3.12). We note that Equation 51 includes corrections to Equation 8-30 of [4]. The software in the Appendix to [4] is correct and matches Equation 51 above.

The derivation of Equation 51 presented in [4] requires the truncation of a binomial expansion. This truncation introduces some modeling inaccuracy, which induces a small error when comparing the implementation to simple, completely accurate cases. All common formulations of the gravity gradient torque expressed in terms of $\boldsymbol{J}$ include this error.

3.10 Shape-Dependent SRP Modeling

Unlike the cannonball model for solar radiation pressure, the model provided by TurboProp for Ananke uses a satellite plate model to generate an attitude dependent acceleration and torque. As presented in [20], the SRP acceleration may be expressed as

$$\ddot{\boldsymbol{r}}_{\text{SRP}} = -P(\boldsymbol{r}) \sum_{k=1}^{n} \frac{A_k}{M} \cos\phi_k \boldsymbol{s}_{k,i} \tag{53}$$

$$\boldsymbol{s}_{k,i} = (1-\rho_k)\hat{r}_{\odot s} + 2\left(\frac{\delta_k}{3} + \rho_k \cos\phi_k\right)\hat{n}_{k,i} \tag{54}$$

where $P(\boldsymbol{r})$ is the pressure at $\boldsymbol{r}$, A_k, ρ_k, and δ_k are the area, specular reflection coefficient, and diffuse coefficient, respectively, for the k-th plate, $\hat{n}_{k,i}$ is the normal vector to the k-th plate in the inertial frame, and $\hat{r}_{\odot s}$ is the unit vector from the center of the plate to the Sun. Given this force, the torque is then

$$\boldsymbol{m}_{\text{SRP}} = -P(\boldsymbol{r}) \sum_{k=1}^{n} A_k \cos\phi_k \left(\boldsymbol{\rho}_{k,b} \times T_b^i \boldsymbol{s}_{k,i}\right), \tag{55}$$

where $\boldsymbol{\rho}_{k,b}$ is the location of the plate's center in the body frame. Although it is not done in the current implementation due to time constraints, the ERP model presented in Section 3.6 may also be formulated using this shape-dependent model.

The satellite structure is provided to the derivative function through an input body file. This file contains information on the plates used to represent its shape and the moment of inertia ($\boldsymbol{J}$) for the satellite. The file is split into three sections: (a) the header, (b) the moment of inertia tensor $\boldsymbol{J}$ and (c) the individual plates that constitute the model. The two-line header, described in Table 5, provides metadata on the file and the total mass of the satellite. The second section, which is nine lines, contains the elements of $\boldsymbol{J}$. A description of the file format for this section may be found in Table 6. Finally, the remaining lines describe the locations and orientations of the individual plates in the model. The number of plates was provided in the header, and Table 7 describes the format of these entries. An example file, `ggSat.bod`, is provided in the `TurboProp/Data/` directory.

Table 5. Header Format for Satellite Body Model Files

C Format Strings	Parameter Description
`%d`	Number of Plates
`%e`	Satellite Total Mass (kg)

3.11 GCRF/ITRF Transformation

This section describes the elements that must be considered when modeling the coordinate transformation between the Earth-fixed frame and the Earth-centered inertial frame. The discussion follows the one presented in [21], which compared the effects of modeling truncation on the accuracy of orbit propagation.

Table 6. Moment of Inertial Line Format for Satellite Body Model Files

C format string: `"%d %d %e"`	
Parameter Description	Format
Index n	Integer
Index m	Integer
Moment of Inertia Tensor Term J_{nm}	Scientific Notation

Table 7. Data Line Format for Satellite Body Model Files

C format string: `"%e, %e, %e, %e, %e, %e, %e, %e, %e"`	
Parameter Description	Format
Plate Area (m)	Scientific Notation
Specular Coefficient	Scientific Notation
Diffusion Coefficient	Scientific Notation
Plate X Position (m) in Satellite Body Frame	Scientific Notation
Plate Y Position (m) in Satellite Body Frame	Scientific Notation
Plate Z Position (m) in Satellite Body Frame	Scientific Notation
Plate Unit Normal Vector X-Component in Satellite Body Frame	Scientific Notation
Plate Unit Normal Vector Y-Component in Satellite Body Frame	Scientific Notation
Plate Unit Normal Vector Z-Component in Satellite Body Frame	Scientific Notation

Satellite operations requiring ever-increasing position accuracy, such as Earth science missions, are on the rise. Additionally, software utilizing special perturbations for orbit propagation is rapidly replacing routines using general perturbations. These numerical models and precise position solutions require accurate frame transformations, particularly between the Geocentric Celestial Reference Frame (GCRF) and the International Terrestrial Reference Frame (ITRF) (i.e., inertial i and fixed e). The procedure and models needed to transform between the GCRF and ITRF are maintained by the International Earth Rotation Service (IERS) [3]. Earth orientation parameters (EOP) are crucial for correctly executing these frame transformations, affecting parameters such as station coordinates, satellite positions, and non-spherical gravitational acceleration vectors. EOPs consist of the following [3]:

- Pole Coordinates (x_p,y_p): coordinates of the Celestial Intermediate Pole (CIP) with respect to the IERS Reference Pole (IRP) in the International Terrestrial Reference System (ITRS). The IRP is the location of the agreed upon terrestrial pole while the CIP is the actual axis of Earth rotation.

- Celestial Pole Offsets (dX,dY): observed corrections to the conventional celestial pole. The conventional celestial pole position is defined by the IAU Precession and Nutation models.

- UT1 Time Difference ($\Delta UT1$): the offset of Universal Time (UT1) from Universal Coordinated Time (UTC), *i.e.* $\Delta UT1 = UT1 - UTC$.

- Length of Day (LOD): time difference between the observed duration of a mean solar day and 86,400 SI secs.
- Atomic Time Offset (ΔAT): time difference between International Atomic Time (TAI) and Universal Coordinated Time (UTC), *i.e.* $\Delta AT = TAI - UTC$.

Although the Atomic Time offset is not technically an EOP, it is included in this list because this value is commonly incorporated into tabulated EOP data files. EOPs are published by the IERS once per day, effective at 0^{h} UTC of that day. These daily EOP values must be interpolated for maximum accuracy at other times during the day. In literature to date, however, recommended interpolation methods to achieve specific accuracies are not mentioned. Additionally, the published values of the pole coordinates, UT1 time difference, and length of day are "tide-free", meaning that users requiring high-precision need to apply additional corrections for diurnal and semi-diurnal ocean tides and libration after the parameter has been interpolated.[3] This fact is fairly unpublicized within astrodynamics literature [5, 6].

As mentioned, EOPs are needed to accurately transform from the ITRF to the GCRF and vise versa. Effective Jan 1, 2009, the IERS recommends the use of the new International Astronomical Union (IAU) models for nutation and precession to perform this GCRF/ITRF transformation.[3, 22, 23, 24, 25, 26, 27] The new model, as a whole, is called the IAU 2000A$_{\text{R06}}$/2006 model. This includes the IAU 2000A$_{\text{R06}}$ nutation theory and the IAU 2006 precession theory. Several methods for implementing this new model have been developed over the past few years, but are all within the uncertainty of the IAU model itself [26, 25, 5, 28]. The CIO-based (Celestial Intermediate Origin) series method of the IAU 2000A$_{\text{R06}}$/2006 model is utilized to perform the GCRF/ITRF transformations for this software. Equations (56–60) below describe the general process of this transformation and more details on the IAU model and implementation processes can be found in [3, 5, 28].

$$\left[\boldsymbol{W}\right] = \text{ROT3}(-s')\text{ROT2}(x_p)\text{ROT1}(y_p) \tag{56}$$

$$\left[\boldsymbol{R}\right] = \text{ROT3}(-\theta_{ERA}) \tag{57}$$

$$\left[\boldsymbol{PN}\right] = \begin{bmatrix} 1-aX^2 & -aXY & X \\ -aXY & 1-aY^2 & Y \\ -X & -Y & 1-a(X^2+Y^2) \end{bmatrix} \text{ROT3}(s) \tag{58}$$

$$\boldsymbol{r}_{GCRF} = \left[\boldsymbol{PN}\right]\left[\boldsymbol{R}\right]\left[\boldsymbol{W}\right]\boldsymbol{r}_{ITRF} \tag{59}$$

$$\dot{\boldsymbol{r}}_{GCRF} = \left[\boldsymbol{PN}\right]\left[\boldsymbol{R}\right]\left\{\left[\boldsymbol{W}\right]\dot{\boldsymbol{r}}_{ITRF} + \boldsymbol{\omega}_{\oplus} \times \left[\boldsymbol{W}\right]\boldsymbol{r}_{ITRF}\right\} \tag{60}$$

For ease of notation in other sections of this document,

$$\boldsymbol{T}_i^e = \left[\boldsymbol{PN}\right]\left[\boldsymbol{R}\right]\left[\boldsymbol{W}.\right] \tag{61}$$

Figure 3 below identifies which EOP contributes to each of the components needed for the frame transformation. To be in full compliance with the models of the IERS Conventions (2010), namely the IAU 2000A$_{\text{R06}}$/2006 model, the pole coordinates, UT1 time difference, and length of day must first be interpolated to the appropriate time and then modified by ocean tide corrections

and libr ›sted by
the IER current
implem ffect on
satellite

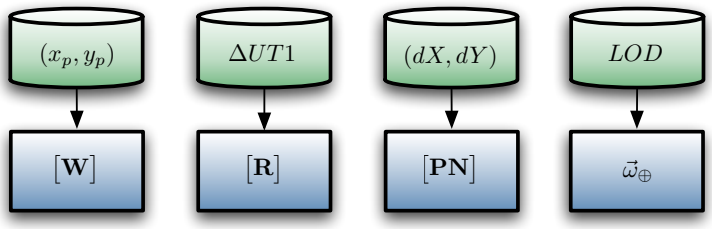

Figure 3. Depiction of Which EOP is used to Generate Each Element in the Transformation Process.

$$(x_p, y_p) = (x_p, y_p)_{\text{IERS}} + (\Delta x, \Delta y)_{\text{ocean tides}} \tag{62a}$$

$$\Delta UT1 = \Delta UT1_{\text{IERS}} + \Delta UT1_{\text{ocean tides}} \tag{62b}$$

$$LOD = LOD_{\text{IERS}} + \Delta LOD_{\text{ocean tides}} \tag{62c}$$

The libration corrections, $(\Delta x, \Delta y)_{\text{libration}}$, are not shown in Equation (62) and are not included in this software for two reasons: 1) they are an order of magnitude smaller than the ocean tide corrections and 2) the model has not been verified by observations as of yet. These libration corrections consist of diurnal and semi-diurnal nutations due to external torque, namely luni-solar torque.[3] The corrections, $(\Delta x, \Delta y)_{\text{ocean tides}}$, include diurnal and semi-diurnal variations caused by ocean tides for the three EOPs in Equation (62) [3].

The subscript "IERS" indicates the daily published values that have been interpolated. These parameters are published from several sources, including the IERS, National Geospatial-Intelligence Agency (NGA), and the United States Naval Observatory (USNO). However, CelesTrak has compiled EOPs from all available sources to create a single file containing EOP data from 1962 up to predictions 1 year into the future.[1] The file maintained by CelesTrak is used by Analytical Graphics Inc. Satellite Tool Kit (STK), and TurboProp requires a periodic update of this file. Tools are provided for this, and are executed as part of the installation software.

The process of interpolating EOPs and adding corrections is outlined by the flowchart shown in Figure 4. It is prudent to remember that the first step is to interpolate any EOP of interest. The computation of the ocean tide corrections is relatively simple and only requires an input of Julian Centuries of Terrestrial Time, T_{TT}. The IERS Conventions provide the algorithm for computing the ocean tide corrections using a table of amplitudes and arguments for 71 tidal components and FORTRAN code is available online from the IERS EOP Product Center [3]. Two different source code files named `INTERP.F`[2] and `ORTHO_EOP.F`[3] are available online for the computation of ocean tide corrections. The file `ORTHO_EOP.F` is based on the full model from [29] and the file

[1] `http://www.celestrak.com/SpaceData/`

[2] `INTERP.F` available here: `ftp://hpiers.obspm.fr/eop-pc/models/interp.f`

[3] `ORTHO_EOP.F` available here: `ftp://tai.bipm.org/iers/conv2010/chapter8/ORTHO_EOP.F`

INTER · two routines
agree w · UT1 [3]. The
implem

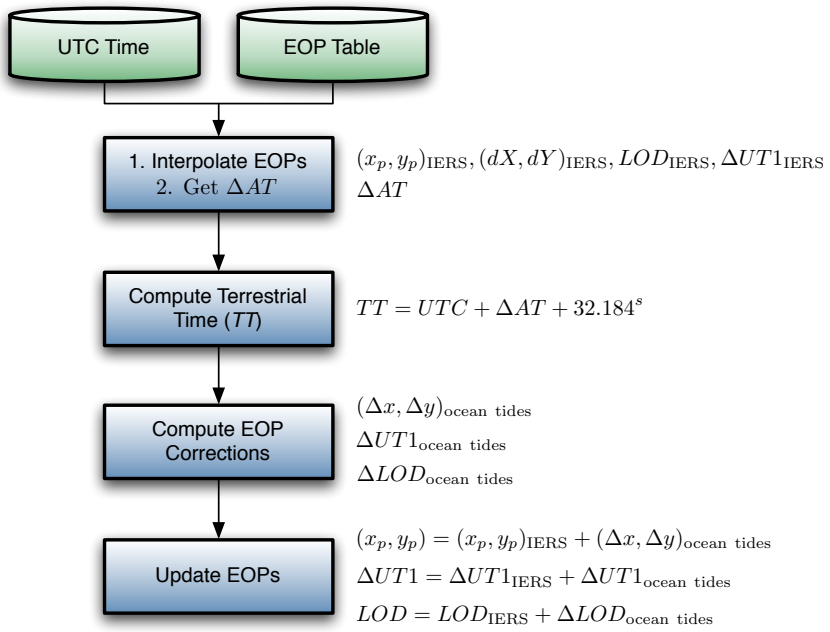

Figure 4. Flowchart of EOP Interpolation and Ocean Tide Correction Process.

The `INTERP.F` routine, mentioned above, also incorporates EOP interpolation into its procedure. The default is a 4-point window Lagrangian interpolation (i.e., 3$^{\text{rd}}$-order Lagrange). Although this is the default interpolation method, it does not mean it is the most accurate. [6] suggests that using a quadratic polynomial interpolation for the pole coordinates and $\Delta UT1$ will yield sufficient accuracy, and [30] suggests that linear interpolation is a common standard. Various methods of interpolation were compared in [21], with this implementation leveraging this work.

As shown in Figure 5 below, corrections are only applied to the pole coordinates, $UT1$ time offset, and length of day parameters. The celestial pole offsets are *observed* corrections to the precession-nutation theory. The corrections are oscillatory as would be expected from ocean tides and are quite distinct. The time window in Figure 5 has been reduced to one day to clearly show the effect of the diurnal and semi-diurnal ocean tide corrections. The corrections to $\Delta UT1$ have a RMS amplitude of about 25 μsec and reach as high as 73 μsec in amplitude during the 3-month period of Jan 1 to Apr 1, 2011.

It should be noted that high-rate EOP estimation (sub-daily) is another field of research that is ongoing. The models described and used in TurboProp are constantly in the process of being verified and improved by research groups performing EOP estimation from Global Positioning System (GPS) and Very-Long Baseline Interferometry (VLBI) measurements.[31, 32, 30] It is important to be mindful of the accuracy of each model and keep track of progress being made on these fronts, because it directly impacts precise frame transformations [21].

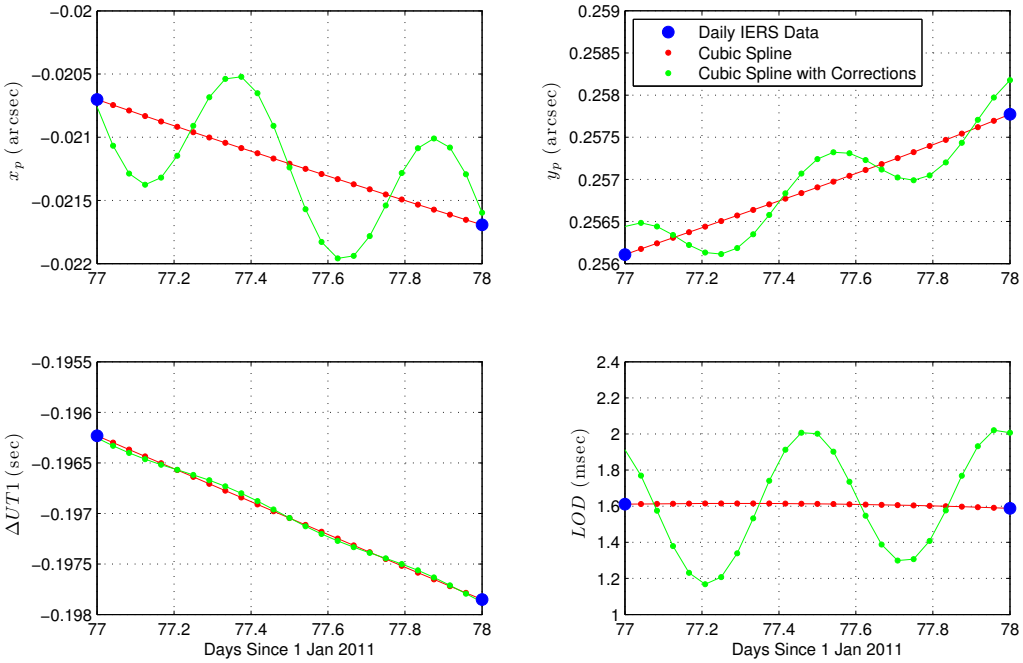

Figure 5. Ocean tide corrections for applicable EOPs on 19 Mar 2011.

3.12 TurboProp/Anake Interface

As mentioned previously, TurboProp provides an interface that may be used in a separate MATLAB integrator for the modeling of the principle forces and torques acting on a satellite. The software provides the models, written in C, and a MEX interface that may be used to access the functions from MATLAB. Extensive details on the inputs may be found in the CU-TurboProp manual supplied with the software.

An example execution of the model has been provided in the sample code `SDTSample.m`. The principle MATLAB call is:

```
dY = deriv_mex( 'SixDOF_Full', time, Y, extras )
```

where `time` is the time of the input state `Y`, the `extras` structure provides parameters needed for modeling the forces and torques, and `dY` is an array populated by $\dot{Y} = F(t, Y)$. Population of the `extras.reftime` parameter may require evaluation of the `UTC2JED()` function to convert to ephemeris time. A full description may be found in the user's manual, and example uses are provided in the sample code.

Also, this software requires internal initialization, i.e. the loading of several data files describing the force model environment, etc. The current version uses a newer implementation that maintains the state of the software with each call of the `deriv_mex()` function. To clear this persistent memory or reinitialize the software, the user must first call:

```
clear deriv_mex
```

to clear the current memory.

As part of Ananke, CCAR developed a derivative function compatible with the bidirectional reflectance distribution function (BRDF) software developed by Pacific Defense Solutions, LLC. The BRDF software is written in MATLAB, and cannot easily be called from TurboProp without: (1) porting the software to C, or (2) calling MATLAB code through an engine running on a separate thread. Hence, we decided to not directly interface TurboProp with the BRDF model. Instead, within the MATLAB-level derivative function, the TurboProp software will be called first, followed by the BRDF-specific function. For this, we define a new derivative function, `SixDOF_Full_BRDF`, that should be called when running with this model. Below is a description of the interface.

`SixDOF_Full_BRDF` is a 6-DOF propagator for both the attitude and translation state of a satellite, and includes perturbations from the aspherical gravity field, atmospheric drag, and third-body effects. The modeled torques include those induced by gravity-gradient. It is assumed that solar radiation pressure and other forces/torques that are dependent on satellite surface properties will be handled by the BRDF. The state, `y0`, is a 14×1 vector:

`y0( 1)`	x position (km)
`y0( 2)`	y position (km)
`y0( 3)`	z position (km)
`y0( 4)`	$\dot{x}$ velocity (km/sec)
`y0( 5)`	$\dot{y}$ velocity (km/sec)
`y0( 6)`	$\dot{z}$ velocity (km/sec)
`y0( 7)`	q_0 scalar part of quaternion
`y0( 8)`	q_1 component of quaternion vector portion
`y0( 9)`	q_2 component of quaternion vector portion
`y0(10)`	q_3 component of quaternion vector portion
`y0(11)`	ω_1 angular velocity in body 1 axis (rad/sec)
`y0(12)`	ω_2 angular velocity in body 2 axis (rad/sec)
`y0(13)`	ω_3 angular velocity in body 3 axis (rad/sec)
`y0(14)`	C_D coefficient of drag (non-dimensional)

Position and velocity coordinates are specified in the GCRF frame centered at the central body, while the quaternion $\bar{q}$ describes the transformation from the GCRF frame to the satellite structure frame. The angular velocity vector $\boldsymbol{\omega}$ describes the rotation rate of the body relative to the inertial frame, and is expressed in the structure frame. The input time is in seconds past the `extras.reftime`.

The origin of the coordinate frame is at the center of mass of the primary body. `extras.mu` must be included and should contain μ (in km^3/sec^2), the gravitational parameter of the primary body. The radius of the primary body (in km) must be included in `extras.radius`. Since this model employs the spherical harmonic model, the degree and order of the expansion is included in `extras.degord`. The gravity gradient torques may include perturbations from non-spherical gravity terms. If this is desired, then the degree and order of the variational equations `extras.degordstm` must be nonzero. The gravity model itself ($\bar{C}_{n,m}$ and $\bar{S}_{n,m}$ coefficients) is provided in `extras.gravfile`. To model atmospheric drag, then the appropriate values for the exponential density model are provide in `extras.atmos`. In this case, the reference density is in kg/m^3, and the scale height and reference radius are in km. The area-to-mass ratio used in

the atmospheric drag calculations are in m^2/kg, and is provided to the software in `extras.A_m`. Set `extras.A_m = 0` to not include atmospheric drag. The reference time, in Julian Ephemeris Time (JED), is provided to the function in `extras.reftime`. Utilities are provide in the MATLAB tools (see TurboProp users manual) to facilitate the conversion to JED. Planets to include for third-body perturbations are provided in the `extras.planets` array, while the central body is defined in `extras.center`. If the central body is specified in `extras.planets`, it will not be included in the calculation of third-body perturbations. The positions of the celestial bodies, relative to the central body, are computed using the JPL DE specified in `extras.ephemfile`. Finally, the satellite moment of inertial tensor is provided in `extras.MOI` as a 3×3 matrix in the body frame. *The elements in* `extras.MOI` *must be in units of kg·m^2/rad^2.*

This version of the software also requires the definition of several files to define the rotation from the ITRF and the GCRF. These new elements of the `extras` structure are:

`extras.XYsFile`	File containing the location of the rotation axis in the X-Y plane
`extras.EOPFile`	File containing the parameters required for EOP evaluation.
`extras.LeapSecFile`	Definition of the leap seconds used in time conversions.

A sample definition may be found in the sample execution files provided in TurboProp.

The outputs of this function are different from other TurboProp derivative functions. The outputs are a vector of length 18, which are:

`out( 1)`	$\dot{x}$ velocity (km/sec)
`out( 2)`	$\dot{y}$ velocity (km/sec)
`out( 3)`	$\dot{z}$ velocity (km/sec)
`out( 4)`	$\ddot{x}$ acceleration (km/sec^2)
`out( 5)`	$\ddot{y}$ acceleration (km/sec^2)
`out( 6)`	$\ddot{z}$ acceleration (km/sec^2)
`out( 7)`	$\dot{q}_0$ rate of change for scalar part of quaternion
`out( 8)`	$\dot{q}_1$ rate of change for component of quaternion vector portion
`out( 9)`	$\dot{q}_2$ rate of change for component of quaternion vector portion
`out(10)`	$\dot{q}_3$ rate of change for component of quaternion vector portion
`out(11)`	torque about body 1 axis (N·m)
`out(12)`	torque about body 2 axis (N·m)
`out(13)`	torque about body 3 axis (N·m)
`out(14)`	rate of change for C_D coefficient of drag (non-dimensional, should be zero)
`out(15)`	$x_{s\odot}$ satellite-to-sun vector in inertial frame (km)
`out(16)`	$y_{s\odot}$ satellite-to-sun vector in inertial frame (km)
`out(17)`	$z_{s\odot}$ satellite-to-sun vector in inertial frame (km)
`out(18)`	ν fraction of Sun visible from the satellite, $1 =$ fully illuminated, $0 =$ in shadow

We provide an example interface with the PDS BRDF model in the file `exampleBRDF.m` in the top-level directory of the TurboProp package. Assuming you have access to the PDS software, then you can execute this sample code using `runExampleBRDF.m`. In this case, change the `filePath` variable to point to the directory with the BRDF test cases and make sure the Multiple-Model Adaptive Estimator (MMAE) software (developed by State University of New York, Buffalo) is in the MATLAB path.

4 RESULTS AND DISCUSSION

4.1 Developed Unit Test Cases

The TurboProp software includes a set of unit test cases (UTCs) to exercise various components of the core functionality. The unit tests currently verify the following: ITRF/GCRF transformation, gravity gradient torques, attitude dynamics and solar radiation pressure.

The ITRF/GCRF transformation unit tests verify the EOP and CIP/CIO parameter lookup and interpolation function as expected and also verify the end-to-end transformation code operates correctly (transformation from ITRF to GCRF and back to ITRF). Since the transformation software was originally developed in MATLAB and then translated to C, the unit tests compare the MATLAB and C results. Furthermore the unit tests were used to compare the C implementation of the transformation to STK output.

TurboProp generates gravity gradient torques from the spherical harmonic gravity field and spacecraft inertia tensor as described in Section 3.9. An alternative method models a simple spacecraft as a collection of point masses and calculates the gravity gradient torque as the sum of the torques from each point [33]. The unit test driver computes the gravity gradient torques via both methods for 10,000 random spacecraft locations, and verifies the maximum relative error is 10^{-6} N·m. This difference is expected given the truncation error discussed in Section 3.9.

To verify the implementation of Euler's equations, we compare the propagation to analytic solutions defined under torque-free motion. For example, when given an axially symmetric body with $J_{11} = J_{22} \neq J_{33}$ (other elements zero), then

$$\boldsymbol{\omega}(t) = \begin{bmatrix} \cos(\omega_p t) & -\sin(\omega_p t) & 0 \\ \sin(\omega_p t) & \cos(\omega_p t) & 0 \\ 0 & 0 & 1 \end{bmatrix} \boldsymbol{\omega}(t_0) \tag{63}$$

where

$$\omega_p = \left(\frac{J_{33}}{J_{11}} - 1 \right) \omega_3. \tag{64}$$

We then compare the numerically propagated $\boldsymbol{\omega}$ using Euler's equations and TurboProp to the solution generated using the this analytic solution. This case is tested using 10,000 random initial conditions to provide more confidence in the result. Tests demonstrate a relative accuracy of at least 10^{-13}, which matches the expected result after floating point error accumulation with numerical integration with a sufficiently long time span.

Unfortunately, validation of the SRP and satellite shape model software requires more complexity. The UTCs developed for the SRP software consider two models: (1) a satellite with 12,800 faces to create an approximate sphere, and (2) a flat plate with the normal vector parallel to

$\boldsymbol{r}_{sat,\odot}$. In the first case, the UTC demonstrates that the model approximates the cannonball model to an accuracy of 10^{-10}. In the second case matches the cannonball model to a relative accuracy of 10^{-13}. Both of these accuracies are computed over 10,000 random initial conditions. In the first test, the orientation of the modeled satellite is randomly varied. In test (2), the location of the plate in Earth orbit is randomly chosen.

4.2 Comparison to MMAE Propagator

In the process of integrating the TurboProp software with the Ananke simulation, we also compared to the default propagator included with the MMAE filter. The MMAE filter included the BRDF software previously mentioned, and provided an additional comparison to ensure the TurboProp-BRDF interface functions properly. Through this process, CCAR assisted in improving the force models included in the MMAE filter.

4.3 Comparisons to Satellite Tool Kit (STK)

Satellite Tool Kit (STK) was used to provide independent validation of various TurboProp components such as: translational state propagation, rotational state propagation, spherical harmonic gravity field, third body gravity, JPL ephemeris, ITRF/GCRF transformation and gravity gradient torque. However it is not possible to configure STK to model all of the forces TurboProp includes, nor is it always possible to force STK to model some forces in the same manner as TurboProp. The primary limitations of the STK validation are that STK does not couple rotation and translation, STK can only include two-body gravity gradient effects and it is difficult to mimic the TurboProp SRP and drag models in STK.

The comparison scenario was based on an object in near geostationary orbit with the body and inertial coordinates initially aligned. The object's initial rotational velocity in all three axes was non-zero and the start of the simulation was Julian day 2455197.516765046. The scenario was propagated for seven days using a Dormand-Prince 8(7) [34] integrator in STK and TurboProp.

The force model for both STK and TurboProp included a degree and order 30 EGM2008 tide free spherical harmonic gravity field, two-body gravity gravity gradient, and third body gravity from the Sun, Moon and Jupiter. The force model did not include drag, SRP or translation/rotation coupling. The simulations used the JPL DE405 ephemeris and the inertia tensor was fully populated (no zero elements) with a mix of positive and negative products of inertia.

Figure 6 shows the difference between STK and TurboProp for both the translational and rotational states. The translational states are shown in radial, in-track and cross-track (RIC) coordinates and the angular velocity is expressed in the body frame. The maximum RSS position error over seven days was 25 mm (approximately $10^{-8}\%$ relative error) and the maximum angular velocity RSS error was 1.8×10^{-8} deg/sec (approximately $10^{-3}\%$ relative error). The disagreement in position is largely due to the inclusion of third body gravity (the error drops by an order of magnitude when ignoring third body gravity). The angular velocity is different in that the increase in error is not linear; rather, it increases by an order of magnitude approximately every 2-3 days (the maximum relative error is $10^{-5}\%$ after 1 day). The angular velocity difference also seems to be more heavily tied to integration step size and likely derives from round-off and truncation error.

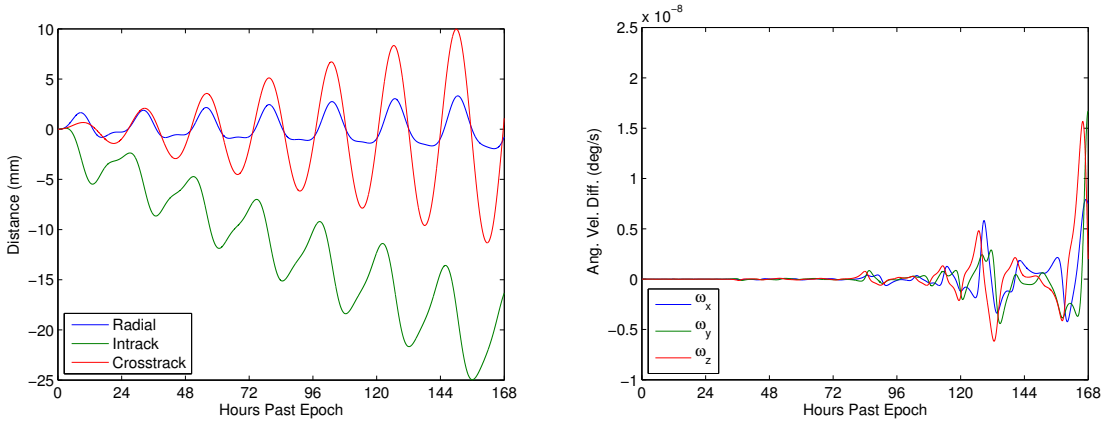

Figure 6. STK vs. TurboProp Radial, In-track and Cross-track Differences (left) and Angular Velocity Differences (right)

5 CONCLUSIONS

This document described the work performed as part of the Ananke simulation development. This work included the addition of higher-fidelity models in CU-TurboProp and validation of the new models, each of which were described in the document. The software interface for the Ananke simulation tool was described, and validation results were presented. All results met required and expected accuracies in the tests considered.

Future work could take several forms. As briefly mentioned in the overview of CU-TurboProp, the software includes several numerical integration routines. Some work could be done to develop improved methods to reduce the computation time required for orbit propagation. One example includes the BLC-IRK integrator in development at CCAR [35, 36]. Additionally, CU-TurboProp may be further improved by adding a liquid tide model, which would improve accuracy for low-Earth orbit propagation, and the modeling of geomagnetic torques.

REFERENCES

[1] Jones, B. A., Born, G. H., and Beylkin, G., "Comparisons of the Cubed-Sphere Gravity Model with the Spherical Harmonics," *Journal of Guidance, Control, and Dynamics*, Vol. 33, No. 2, March-April 2010, pp. 415–425.

[2] Jones, B. A., Born, G. H., and Beylkin, G., "Sequential Orbit Determination with the Cubed-Sphere Gravity Model," *Journal of Spacecraft and Rockets*, Vol. 49, No. 1, Jan.-Feb. 2012, pp. 145–156.

[3] Petit, G. and Luzum, B., "IERS Conventions (2010)," IERS Technical Note 36, International Earth Rotation and Reference Systems Service (IERS), Frankfurt am Main, Germany, 2010.

[4] Gottlieb, R. G., "Fast Gravity, Gravity Partials, Normalized Gravity, Gravity Gradient Torque and Magnetic Field: Derivation, Code and Data," Tech. Rep. NASA Contractor Report 188243, NASA Lyndon B. Johnson Space Center, Houston, TX, February 1993.

[5] Vallado, D. A. and McClain, W. D., *Fundamentals of Astrodynamics and Applications*, Microcosm Press and Springer, Hawthorne, CA and New York, NY, 3rd ed., 2007.

[6] Montenbruck, O. and Gill, E., *Satellite Orbits: Models, Methods, Applications*, Springer, Berlin Heidelberg New York, 2005.

[7] Tapley, B. D., Schutz, B. E., and Born, G. H., *Statistical Orbit Determination*, Elsevier Academic Press, Burlington, MA, 1st ed., 2004.

[8] Lundberg, J. B. and Schutz, B. E., "Recursion Formulas of Legendre Functions for Use with Nonsingular Geopotential Models," *Journal of Guidance*, Vol. 11, No. 1, Jan.-Feb. 1988, pp. 31–38.

[9] Tapley, B. D., Ries, J. C., Bettadpur, S. V., Chambers, D., Cheng, M., Condi, F., and Poole, S., "The GGM03 Mean Earth Gravity Model from GRACE," *American Geophysical Union, Fall Meeting*, Abstract No. G42A-03, 2007.

[10] Pavlis, N. K., Holmes, S. A., Kenyon, S. C., and Factor, J. K., "An Earth Gravitational Model to Degree 2160: EGM2008," *Proceedings of the European Geosciences Union General Assembly*, Vienna, Austria, April 13-18 2008.

[11] Lemoine, F. G., Kenyon, S. C., Factor, J. K., Trimmer, R. G., Pavlis, N. K., Chinn, D. S., Cox, C. M., Klosko, S. M., Luthcke, S. B., Torrence, M. H., Yand, Y. M., Williamson, R. G., Pavlis, E. C., Rapp, R. H., and Olson, T. R., "The Development of the Joint NASA GSFC and NIMA Geopotential Model EGM96," Tech. Rep. NASA/TP-1998-206861, NASA Goddard Space Flight Center, Greenbelt, Maryland, 20771, USA, July 1998.

[12] Tapley, B. D., Watkins, M. M., Ries, J. C., Davis, G. W., Eanes, R. J., Poole, S. R., Rim, H. J., Schutz, B. E., Shum, C., Nerem, R. S., Lerch, F. J., Marshall, J. A., Klosko, S. M., Pavlis, N. K., and Williamson, R. W., "The Joint Gravity Model 3," *Journal of Geophysical Research*, Vol. 101(B12), 1996, pp. 28,029–28,050.

[13] NGA, "Department of Defense World Geodetic System 1984, Its Definition and Relationships With Local Geodetic Systems," Tech. Rep. TR 8350.2, National Geospatial-Intelligence Agency, January 2000.

[14] Standish, E. M., Newhall, X. X., Williams, J. G., and Folkner, W. M., "JPL Planetary and Lunar Ephemerides, DE403/LE403," Interoffice memorandum IOM 314.10-127, Jet Propulsion Laboratory, May 22 1995.

[15] Standish, E. M., "JPL Planetary and Lunar Ephemerides, DE405/LE405," Interoffice memorandum IOM 312F-98-048, Jet Propulsion Laboratory, August 26 1998.

[16] Folkner, W. M., Williams, J. G., and Boggs, D. H., "The Planetary and Lunar Ephemeris DE421," IPN Progress Report 42-178, Jet Propulsion Laboratory, California Institute of Technology, http://ipnpr.jpl.nasa.gov/progress_report/42-178/178C.pdf, August 2009.

[17] Knocke, P. C., Ries, J. C., and Tapley, B. D., "Earth Radiation Pressure Effects on Satellites," *AIAA/AAS Astrodynamics Specialist Conference*, Minneapolis, Minnesota, August 15-17 1988.

[18] Schaub, H. and Junkins, J. L., *Analytical Mechanics of Space Systems*, American Institute of Aeronautics and Astronautics, Reston, VA, 2nd ed., 2009.

[19] Kuipers, J. B., *Quaternions and Rotation Sequences*, Princeton University Press, Princeton, New Jersey, 1999.

[20] Hughes, P. C., *Spacecraft Attitude Dynamics*, John Wiley and Sons, Inc., New York, 1986.

[21] Bradley, B. K., Vallado, D. A., Sibois, A., and Axelrad, P., "Earth Orientation Parameter Consideration for Precise Spacecraft Operations," *AAS/AIAA Astrodynamics Specialist Conference*, Girdwood, AK, July 31 - August 4 2011.

[22] Mathews, P. M., Herring, T. A., and Buffet, B. A., "Modeling of nutation and precession: New nutation series for nonrigid Earth and insights into the Earth's interior," *Journal of Geophysical Research: Solid Earth*, Vol. 107, No. B4, April 2002, pp. ETG 3–1–ETG 3.26.

[23] Buffett, B. A., Mathews, P. M., and Herring, T. A., "Modeling of nutation and precession: Effects of electromagnetic coupling," *Journal of Geophysical Research: Solid Earth*, Vol. 107, No. B4, April 2002, pp. ETG 5–1 – ETG 5–14.

[24] Herring, T. A., Mathews, P. M., and Buffet, B. A., "Modeling of nutation-precession: Very lon baseline interferometry," *Journal of Geophysical Research: Solid Earth*, Vol. 107, No. B4, April 2002, pp. ETG 4–1 – ETG 4–12.

[25] Hilton, J. L., Capitaine, N., Chapront, J., Ferrandiz, J. M., Fienga, A., Fukushima, T., Getino, J., Mathews, P., Simon, J.-L., Soffel, M., Vondrak, J., Wallace, P., and Williams, J., "Report of the International Astronomical Union Devision I Working Group on Precession and the Ecliptic," *Celestial Mechanics and Dynamical Astronomy*, Vol. 94, No. 3, 2006, pp. 351–367.

[26] Capitaine, N. and Wallace, P. T., "Concise CIO based precession-nutation formulations," *Astronomy and Astrophysics*, Vol. 478, No. 1, January 2008, pp. 277–284.

[27] Fukushima, T., "A New Precession Formula," *The Astronomical Journal*, Vol. 126, No. 1, 2003, pp. 494–534.

[28] Coppola, V., Seago, J. H., and Vallado, D. A., "The IAU 200A and IAU 2006 Precession-Nutation Theories and Their Implementation," *AAS/AIAA Astrodynamics Specialist Conference*, Pittsburgh, PA, August 9-13 2009.

[29] Ray, R. D., Steinberg, D. J., Caho, B. F., and Cartwright, D. E., "Diurnal and Semidiurnal Variations in the Earth's Rotation Rate Induced by Oceanic Tides," *Science*, Vol. 264, No. 5160, May 6 1994, pp. 830–832.

[30] Artz, T., Bernhard, L., Nothnagel, A., Steigenberger, P., and Tesmer, S., "Methodology for the combination of sub-daily Earth rotation from GPS and BLBI observations," *Journal of Geodesy*, Vol. 86, No. 3, March 2012, pp. 221–239.

[31] Kouba, J., "Sub-Daily Earth Rotation Parameters and the International GPS Service Orbit/Clock Solution Products," *Studia Geophysica et Geodaetica*, Vol. 46, No. 1, January 2002, pp. 9–25.

[32] Artz, T., B ockmann, S., Nothnagel, A., and Steigenberger, P., "Subdiurnal variations in the Earth's rotation from continuous Very Long Baseline Interferometry campaigns," *Journal of Geophysical Research: Solid Earth*, Vol. 115, No. B5, May 2010, pp. B05404.

[33] Thompson, B. F., Hammen, D. G., Jackson, A. A., and Crues, E. Z., "Validation of Gravity Acceleration and Torque Algorithms for Astrodynamics," *18th Annual AAS/AIAA Spaceflight Mechanics Meeting*, Galveston, Texas, January 28 - 31 2008.

[34] Prince, R. J. and Dormand, J. R., "High order embedded Runge-Kutta formulae," *Journal of Computational and Applied Mathematics*, Vol. 7, No. 1, March 1981, pp. 67–75.

[35] Beylkin, G. and Sandberg, K., "ODE Solvers Using Bandlimited Approximations," Under review, preprint at http://arxiv.org/abs/1208.3285, 2012.

[36] Bradley, B. K., Jones, B. A., Beylkin, G., and Axelrad, P., "A New Numerical Integration Technique in Astrodynamics," *22nd Annual AAS/AIAA Space Flight Mechanics Meeting*, Charleston, SC, Jan. 29 - Feb. 2 2012.

LIST OF SYMBOLS, ABBREVIATIONS, AND ACRONYMS

A	Area
$\bar{A}_{n,m}$	Derived Legendre function of degree n and order m
BRDF	Bidirectional Reflectance Distribution Function
$C_{n,m}, S_{n,m}$	Stokes coefficients
CCAR	Colorado Center for Astrodynamics Research
CIO	Celestial Intermediate Origin
CIP	Celestial Intermediate Pole
CU	University of Colorado
DE	Design Ephemeris
dX, dY	Celestial pole offsets
EGM	Earth Gravity Model
EOP	Earth Orientation Parameter
ERP	Earth Radiation Pressure
F	Force model
GCRF	Geocentric Celestial Reference Frame
GR	General Relativity
GGM	GRACE Gravity Model
GP	Gravity Perturbations
GPS	Global Positioning System
I_f	In-phase amplitude of tide f
IAU	International Astronautical Union
IERS	International Earth Reference System
IRP	IERS Reference Pole
ITRF	International Terrestrial Reference Frame
J_{ij}	i, i element of J
$\boldsymbol{J}$	Moment of inertia tensor
JGM	Joint Gravity Model
JPL	Jet Propulsion Laboratory
$k_{n,m}$	Geopotential love number for degree/order (n,m)
LOD	Length of Day
M	Mass
m	Spherical harmonics order
$\boldsymbol{m}$	Torque vector
MMAE	Multiple-Model Adaptive Estimator
n	Spherical harmonics degree
O_f	Out-of-Phase amplitude of tide f
ODE	Ordinary Differential Equation
P	Pressure
$\bar{P}_{n,m}$	Associated Legendre function of degree n and order m
PDS	Pacific Defense Solutions
$\boldsymbol{PM}$	Earth precession and nutation matrix
$\bar{q}$	Quaternion

$\boldsymbol{q}$	Vector portion of the quaternion
q_0	Scalar portion of the quaternion
$\boldsymbol{R}$	Earth pole rotation matrix
r	Magnitude of position vector
$\boldsymbol{r}$	Position vector
$\dot{\boldsymbol{r}}$	Velocity vector
$\ddot{\boldsymbol{r}}$	Acceleration vector
RIC	Radial, In-Track, Cross-Track
RMS	Root Mean Square
RSO	Resident space object
RSS	Root Sum Square
SSA	Space Situational Awareness
SET	Solid Earth Tides
SRP	Solar Radiation Pressure
SWIG	Simplified Wrapper and Interface Generator
6-DOF	Six degree of freedom
STK	Satellite Tool Kit
STM	State Transition Matrix
T^i_j	Transformation matrix from frame i to frame j
t	Time
TAI	International Atomic Time
3B	Third-body
2B	Two-body
U	Geopotential
USNO	United States Naval Observatory
UTC	Universal Coordinated Time
UT1	Universal Time
VLBI	Very-Long Baseline Interferometry
$\boldsymbol{W}$	Bias matrix
WGS	World Geodetic System
x, y, z	Cartesian position components
x_p, y_p	Pole coordinates
$\boldsymbol{x}$	State deviation vector
X	State vector
δ_k	diffuse reflection coefficient
λ	Longitude
ω	Angular rate
μ	Gravitation parameter
ρ_k	specular reflection coefficient
$\boldsymbol{\rho}$	Satellite facet location
Φ	State transition matrix (symbol)
ϕ	Geocentric latitude
$\boldsymbol{\omega}$	Angular momentum vector
$\bar{\omega}$	Pure quaternion

DISTRIBUTION LIST

DTIC/OCP
8725 John J. Kingman Rd, Suite 0944
Ft Belvoir, VA 22060-6218 1 cy

AFRL/RVIL
Kirtland AFB, NM 87117-5776 2 cys

Official Record Copy
AFRL/RVSV/Thomas Lovell 1 cy